GaInNAs SESAMs passively mode-locking 1.3-μm solid-state lasers

V. Liverini, S. Schön, R. Grange, M. Haiml, S.C. Zeller and U. Keller

Abstract: A GaInNAs semiconductor saturable absorber mirror (SESAM) is demonstrated that is able to passively mode-lock a 1.3-μm Nd:YLF laser. The mirror was grown by molecular beam epitaxy and consists mainly of a GaInNAs single quantum well on an AlAs/GaAs distributed Bragg reflector. Two designs were grown: resonant and antiresonant. The first favoured optical characterisation, while the second one was more fitted to self-start passive mode-locking in the laser. Rapid thermal annealing was used to tune this wavelength closer to the desired laser wavelength of 1314 nm. Nonlinear characterisation of both designs allowed calculation of the saturation fluence of a 10-nm GaInNAs QW with photoluminescence around 1330 nm independently of design. It was measured to be $3.5 \pm 0.5\ \mu J/cm^2$. The incorporation of about 2% of N in $In_{0.36}Ga_{0.64}As$ red-shifted the as-grown photoluminescence to about 1370 nm. The nonlinear optical characterisation of the antiresonant SESAM showed low saturation fluence ($11.2\ \mu J/cm^2$), low nonsaturable losses and a recovery time suitable for ps-pulse generation. With this SESAM we obtained clean self-starting mode-locking with 6.7-ps pulses at a repetition rate of 117 MHz and a maximum average output power of 580 mW.

1 Introduction

Semiconductor saturable absorber mirrors (SESAMs) are powerful devices able to passively mode-lock solid-state lasers and to suppress Q-switching instabilities [1–4]. They are usually grown monolithically either by molecular beam epitaxy (MBE) or by metalorganic vapour phase epitaxy (MOVPE). Several device designs are possible, however the main components are a distributed Bragg reflector (DBR) and an absorber layer. The ideal DBRs for these devices are GaAs-based ones because the high contrast in the refractive index of their binary materials allows for a smaller layer number in order to obtain high reflectivity, and because their thermal behaviour is better than that of their InP-based DBRs. It is challenging to find good absorbers for the telecommunication wavelengths regime (1.3 and 1.5 μm). So far, InGaAs quantum wells (QWs) have been used, but the high indium concentration required to red-shift the absorption edge to 1.3 μm (more than 40%) makes the material highly mismatched to GaAs-based substrates and therefore highly strained. The consequence is a reduced surface quality with defects, which increase the insertion losses during laser operation [5].

In 1996, Kondow *et al.* discovered that incorporating just a few percent nitrogen in InGaAs to form the quaternary alloy GaInNAs would have two advantages: (i) the wavelength would be drastically red-shifted, and (ii) the lattice-mismatch to GaAs would be reduced [6]. Even though the strain in the QWs is reduced by the introduction of nitrogen, this alloying process also decreases the crystalline quality of the material by introducing new types of defects that are still under investigation [7]. In fact, low photoluminescence (PL) intensities in as-grown GaInNAs QWs posed a big challenge in the fabrication of active devices, such as vertical-cavity surface-emitting lasers (VCESELs) [8]. However, SESAMs are passive devices, which make use of the absorbing properties of the semiconductor material. In this case, nonradiative recombination due to the defects in GaInNAs can be used for fast carrier recombination in the SESAM to allow for the generation of short pulses in a laser. One more interesting characteristic of GaInNAs is its drastic bandgap blue-shift when exposed to annealing [9]. Such behaviour can be used to our advantage to tune the absorption edge to the desired wavelength by post-growth processing.

A GaInNAs SESAM was previously used to mode-lock a quasi-CW-pumped Nd:YLF and Nd:YALO laser at 1.3 μm. However no information on the nonlinear optical characteristics, such as saturation fluence, was given [10]. In contrast, here we provide full characterisation of the nonlinear properties of the SESAMs and demonstrate stable self-starting CW mode-locking operation using a GaInNAs SESAM.

2 Experimental

The growth of the devices was carried out in an Applied EPI Gen III MBE system in which Ga, In and As_2 were provided from solid sources and N radicals were supplied with an RF plasma source. During the growth reflection high-energy electron diffraction (RHEED) was used to monitor the crystallinity of the devices. Since the growth of GaInNAs is normally favoured by relatively low temperatures, we preferred to use a diffuse reflectance spectroscopy (DRS) system in place of a pyrometer to control the growth temperature.

Test structures of InGaAs and GaInNAs single QWs (SQWs) on GaAs substrates were grown before the SESAMs to achieve the optimum growth temperature, the

© IEE, 2004

IEE Proceedings online no. 20040877

doi: 10.1049/ip-opt:20040877

Paper first received 29th April and in revised form 3rd June 2004

The authors are with the Department of Physics, Institute of Quantum Electronics, Swiss Federal Institute of Technology, Zürich, Switzerland and are also with ETH Hönggerberg, Wolfgang-Pauli-Str. 16, CH-8093, Zürich, Switzerland

desired growth rates and stoichiometry. The material properties of these structures, as well as the SESAMs later on, were analysed by (400) X-ray diffraction (XRD) in a $\theta/2\theta$ X-ray diffractometer. The measured rocking curves were fitted according to dynamical diffraction theory. From this analysis we can discover the thickness of the grown layers, the In and N incorporations in the QWs and the perpendicular mismatch with the GaAs substrate. The electronic bandgap energy of the semiconductors grown was measured with a commercial PL system at room temperature to provide us with an approximation to the absorption edge of the material. The samples were excited by a 45-mW, 785-nm laser diode and their PL was collected with an InGaAs detector. The results had a nominal resolution of ± 2 nm. With this system we had also the possibility of mapping the PL throughout the whole wafer to check the homogeneity of the growth. Post-growth processing was carried out in a rapid thermal annealing (RTA) system under constant N_2 flow at temperatures of 550–700°C for one minute. Smaller pieces of the wafer, usually $5 \times 5\,mm^2$, were carefully cleaved and analysed by PL before and after the RTA procedure. Specific samples were also analysed by XRD before and after RTA to monitor the stoichiometry of the QWs.

The optical characterisation was carried out on the SESAMs. A CARY 5E photospectrometer was used to measure the linear reflectivity. For the study of the nonlinear parameters, we performed two experiments using 80-MHz, 280-fs pulses from a commercial optical parametric oscillator (OPO). Degenerate pump-probe experiments were carried out in order to observe the time response of the SESAMs and to ensure that they would be fast enough in the laser. The pump fluence for these experiments was $18\,\mu J/cm^2$ and the probe fluence $0.6\,\mu J/cm^2$. However, nonlinear reflectivity experiments were done to determine the nonlinear parameters, namely, the saturation fluence F_{SAT}, the modulation depth ΔR and the nonsaturable losses ΔR_{ns}.

Finally, we tested the SESAMs by introducing them in a standard delta-cavity laser composed of a Nd:YLF crystal with emission at 1314 nm and a 1.25% output coupler. The laser cavity was pumped by a CW Ti:sapphire laser and was flooded with dry nitrogen to avoid water vapour absorption. Mode-locking was identified with the use of a microwave signal spectrum and an optical spectrum analyser was used to check the optical spectrum. When the SESAMs mode-locked the laser, we measured the pulse duration with an autocorrelation setup, increased the power in steps to find out the Q-switched mode-locking (QML) threshold, and used the microwave spectrum to measure the mode-locking build-up time.

3 Results and discussion

From the MBE growth of the test structures mentioned above, we obtained the desired growth conditions at a temperature of about 450°C for $Ga_{0.64}In_{0.36}N_{0.02}As_{0.98}$ 10-nm SQWs. During the growth of the SQWs, the RHEED showed a streaky pattern, indicating two-dimensional growth. The good quality of the GaInNAs growth can also be seen in the XRD measurements in Fig. 1, where the fringes due to the GaAs cap layer grown on top of the SQWs demonstrate a good interface between the two layers. This Figure also displays the XRD measurements of a 10-nm InGaAs SQW with comparable In concentration, GaAs cap layer, and SQW thickness as well as the fits of both structures (thinner lines). Please note that the offset between

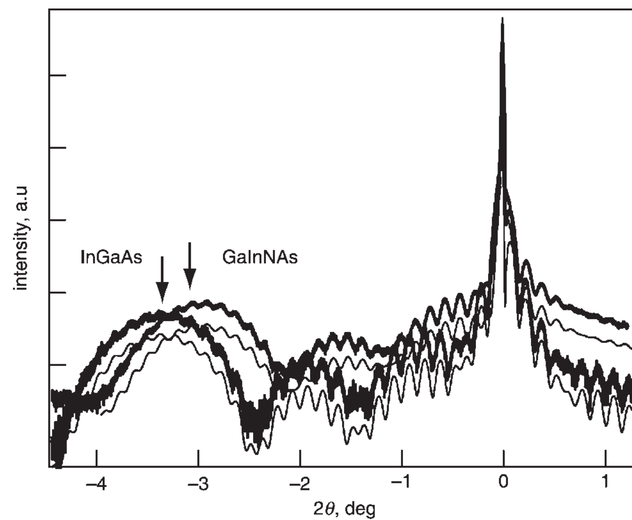

Fig. 1 *XRD measurements of InGaAs SQW and fit (thin line) and XRD of a GaInNAs SQW with similar In concentration and thickness and fit (thin line)*

the measurements and the fits is artificial for illustration purposes. The decrease in mismatch to GaAs is clearly demonstrated by the shift of the GaInNAs QW peak towards the GaAs substrate peak. By using the growth parameters optimised by the growth of the GaInNAs SQW test structures, we grew two GaInNAs SESAM designs: a resonant one with larger modulation depth, which allowed for more accurate nonlinear optical analysis, and an antiresonant one, which was specifically fabricated to meet the requirements of the laser used. Both SESAMs consisted of a 30-pair AlAs/GaAs DBR centred at 1290 nm, a 79-nm GaAs spacer layer and a 10-nm GaInNAs QW. The GaAs cap layer grown on top was 10 nm for the resonant design and 122 nm for the antiresonant design. By comparing the XRD of the SESAMs and that of the DBR on which they were grown, we noticed the appearance of the GaInNAs QW peaks for both designs. The similar position and shape of the QW peaks of the SESAMs indicated that the devices also had similar compositions, namely about 36% In and 2% N.

From the resonant SESAM it is impossible to obtain the PL emission because the resonance in the cavity design alters the PL emission spectrum. The absorption edge was therefore estimated from the test structures. For as-grown samples, the PL of a 10-nm $Ga_{0.64}In_{0.36}N_{0.02}As_{0.98}$ SQW was about 1370 nm. Applying rapid thermal annealing (RTA) under constant N_2 flow at 600°C for 1 min resulted in a blue-shift of about 40 nm and in an improvement in PL intensity, as shown in Fig. 2*a*.

In our studies we have noticed a nearly linear decrease of the PL wavelength with increasing RTA temperature (inset in Fig. 2*a*). However, XRD analysis before and after RTA for the same samples has shown no change in the composition of the QW even at the highest temperature used (700°C) (see Fig. 2*b*). This would indicate that In is not outdiffusing and that some other processes are responsible for the blue-shift experienced.

From the inset in Fig. 2*a* we could extrapolate the RTA temperature, which would blue-shift the absorption edge of the GaInNAs SQW closer to the desired wavelength range (just above 1320 nm). Therefore, we performed RTA on the SESAMs after growth at 600°C for one minute. For the antiresonant design, due to the lack of resonance, we could also measure the PL and confirm that it was in the same range as the test structures.

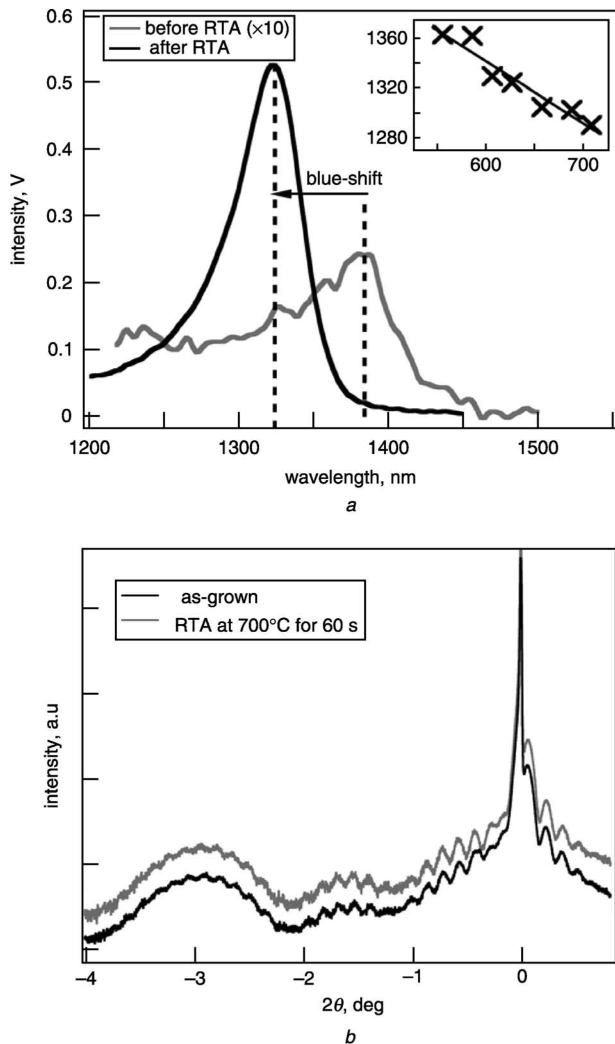

Fig. 2 *PL and XRD data for GaInNAs SQW*

a PL spectra of as-grown GaInNAs SQW with intensity increased by ten times and PL of the same sample after RTA at 600°C for 1 min; Inset: trend of the PL wavelength against RTA temperature for GaInNAs SQW samples with as-grown PL of about 1370 nm (all the RTA experiments were performed for one minute)

b XRD measurements of a GaInNAs SQW sample before and after RTA at 700°C for 1 min (measurements offset with respect to each other for displaying purposes)

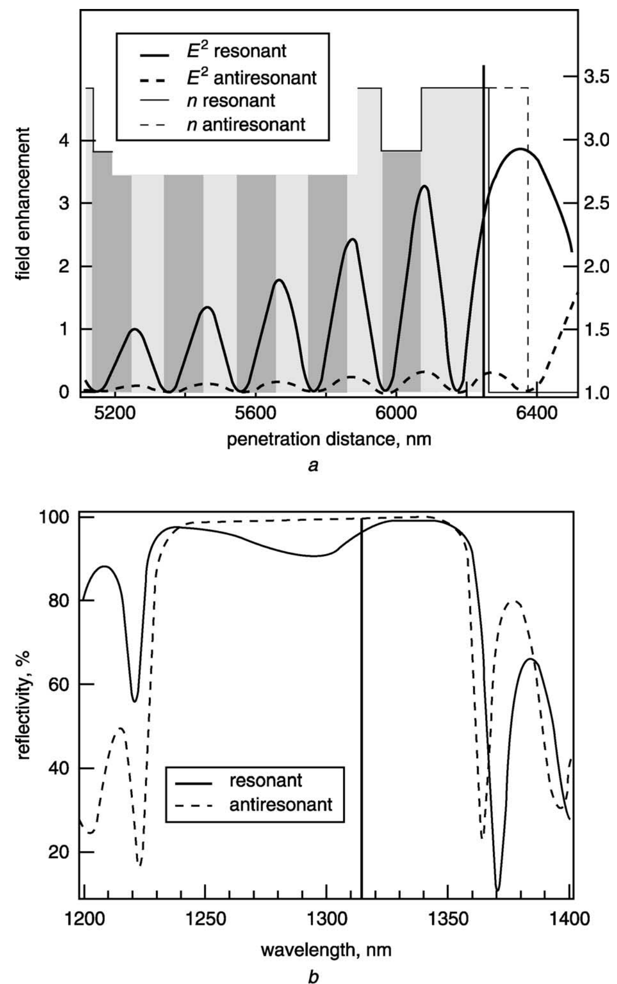

Fig. 3 *Field enhancement and linear reflectivity for resonant and antiresonant SESAMs*

a SESAM design and field intensities

b Linear reflectivity

Field intensities are normalised to the incident field and calculated for the laser wavelength of 1314 nm

The main difference between the two SESAM designs is that the field enhancement in the absorber is much higher in the resonant design than in the antiresonant one. For the same absorber material the saturation fluence scales inversely–linearly and the modulation depth and nonsaturable losses scale linearly with the field enhancement. For our specific designs the field enhancement in the absorber of the resonant SESAM was about nine times larger than in the antiresonant one (Fig. 3*a*). The linear reflectivity obtained shows clearly the resonant dip in the resonant design and the lack thereof in the antiresonant one (Fig. 3*b*).

For both nonlinear optical measurements, the larger modulation depth in the resonant SESAM contributed to a less noisy signal as can be seen in both Figs. 4*a* and 4*b*. Nonetheless, in Fig. 4*a* the trend was the same for both designs, which implies that the absorber materials have indeed the same defect concentration. Both curves could be fitted by a double-exponential decay. The first and faster decay ($\sim$1ps) is attributed to intraband processes such as thermalisation. The slower component, of about 30 ps, is ideally suited for self-starting and stable mode-locking in the picosecond regime [11]. However, for as-grown samples the decay behaviour was faster, which implies that some nonradiative defects were healed in the annealing process.

For the nonlinear reflectivity measurements the results can be seen in Fig. 4*b*. The measured data (crosses) exhibit a strong rollover due to induced absorption, which can be fitted with a model function (solid lines) including this absorption. However, the mode-locked laser only generated ps-pulses for which the rollover occurs at much higher fluences. Therefore, the parameters of the SESAMs were derived from a fit excluding this absorption. We measured a saturation fluence $F_{SAT} = 1\ \mu J/cm^2$, a modulation depth of $\Delta R = 3.9\%$ and nonsaturable losses $\Delta R_{ns} = 0.3\%$. For the antiresonant design, we obtained a saturation fluence $F_{SAT} = 11.2\ \mu J/cm^2$, a modulation depth of $\Delta R = 0.6\%$ and nonsaturable losses $\Delta R_{ns} = 0.04\%$. In comparison 1.3-μm InGaAs antiresonant SESAMs were demonstrated with a saturation fluence of several $100\ \mu J/cm^2$ and much higher nonsaturable losses (up to some percent) [5]. We attribute the very low nonsaturable losses obtained to lower strain in the QW due to the better matching conditions of GaInNAs to the GaAs-based substrate.

Since from our designs we could calculate the field enhancement (0.29 and 2.5 in the antiresonant and resonant SESAMs, respectively), we were then able to use the scaling between the two fields to extrapolate the saturation fluence of a 10-nm GaInNAs QW with PL emission around 1330 nm. We calculated that this should be $3.5 \pm 0.5\ \mu J/cm^2$.

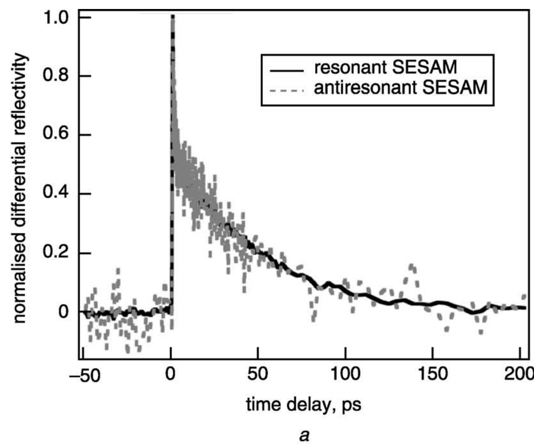

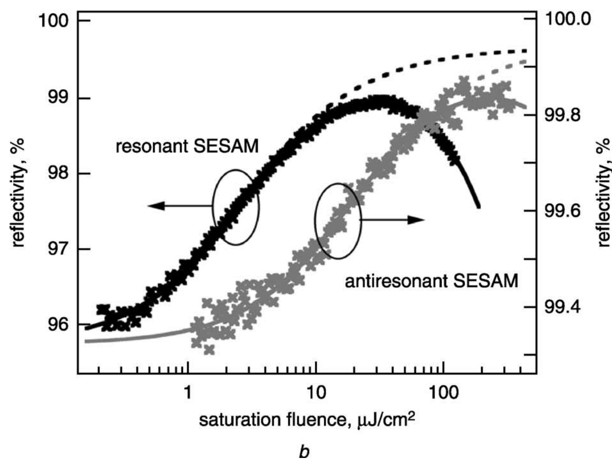

Fig. 4 *Nonlinear optical properties of resonant and antiresonant SESAMs*

a Normalised differential reflectivity of resonant and antiresonant SESAMs

b Nonlinear reflectivity against pulse energy fluence of the resonant SESAM and the antiresonant SESAMs: measured data (crosses, 280-fs pulses, 1314 nm), fit including induced absorption (solid lines), fit excluding induced absorption for longer pulses (dashed lines)

Because of the particular design of the cavity, only the antiresonant SESAM was used to generate mode-locking. Please note that even though the cavity was pumped by a CW Ti:sapphire laser, the same pumping conditions could also be easily achieved with diode pumping. We demonstrated clean self-starting fully passive CW mode-locking with a GaInNAs SESAM. The laser cavity setup used is shown in Fig. 5*a*. We measured a pulse duration as short as 6.7 ps (Fig. 5*b*) fitted with a sech^2 function at an average output power of 520 mW and a repetition rate of 117 MHz. The optical bandwidth of the pulse was 0.39 FWHM giving rise to a time bandwidth product of 0.45. The inset in Fig. 5*b* shows the microwave spectrum of the pulses, which clearly demonstrates clean CW mode-locking with no sidebands, which would be visible with a spacing of some 10 kHz for Q-switched mode-locking (QML), at the repetition rate of 117 MHz. To demonstrate reliable self-starting of CW mode-locking, we measured the build-up time. Pulsed operation started immediately with some spiking behaviour within 100 μs of unblocking the laser cavity. In about 25 ms stable CW mode-locking started. Below 490 mW of output power the laser operated in QML mode, but above this power up to a maximum average power of 580 mW stable CW mode locking was present.

Amazingly enough, the CW mode-locked output power obtained with the SESAM in the laser cavity was only 10% lower than the CW output power obtained with a high reflector. We observed no degradation of the SESAM even after several hours of operation in the CW mode-locking regime. Moreover, the laser spot could be translated over the $5 \times 5\,\mathrm{mm}^2$ SESAM without losing mode-locking. The homogeneity of the sample was also confirmed by the nonlinear optical characterisation, which was invariant throughout the SESAM.

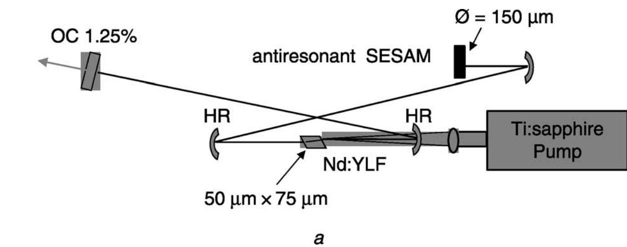

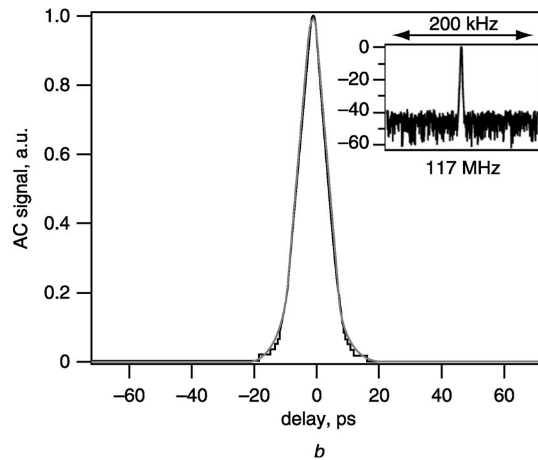

Fig. 5 *Laser cavity setup and laser performance*

a Diagram of the laser cavity mode-locked with the antiresonant GaInNAs SESAM. The spot size on the SESAM is about 150 μm in diameter, and that on the laser crystal is 50 μm × 75 μm

b Laser performance data: intensity autocorrelation of 6.7 ps, data (black line), sech^2-fit (grey line)

Inset: RF spectrum, logarithmic scale (span: 200 kHz, resolution BW: 1 kHz)

4 Conclusions

We attribute the excellent mode-locking results to the use of the novel absorber GaInNAs. The very low nonsaturable losses measured are due to the better matching conditions of GaInNAs to the GaAs-based substrate on which it was epitaxially grown by MBE. Healing some of the defects in the as-grown samples with RTA resulted in slower recombination times, which were, in any case, still in a good range for the generation of picosecond pulses. The low saturation fluence measured is also an excellent material characteristic, which makes this absorber a potential candidate for other applications, such as high-repetition lasers in the telecommunication wavelength regime.

In conclusion, we provide for the first time full nonlinear optical characterisation of GaInNAs SESAMs and demonstrate clean stable self-starting passive CW mode-locking of a Nd:YLF laser with the use of a GaInNAs SESAM. We obtained pulses as short as 6.7 ps at a repetition rate of 117 MHz and a maximum average output power of 580 mW. The laser showed stable mode-locking over several hours and no Q-switching instabilities were observed.

5 Acknowledgments

This work was supported by the NCCR Quantum Photonics program of the Swiss National Science Foundation.

6 References

1 Keller, U., Miller, D.A.B., Boyd, G.D., Chiu, T.H., Ferguson, J.F., and Asom, M.T.: 'Solid-state low-loss intracavity saturable absorber for Nd:YLF lasers: an antiresonant semiconductor Fabry-Perot saturable absorber', *Opt. Lett.*, 1992, **17**, pp. 505–507
2 Keller, U., Weingarten, K.J., Kärtner, F.X., Kopf, D., Braun, B., Jung, I.D., Fluck, R., Hönniger, C., Matuschek, N., and Aus Der Au, J.: 'Semiconductor saturable absorber mirrors (SESAM's) for femtosecond to nanosecond pulse generation in solid-state lasers', *IEEE J. Sel. Top. Quantum Electron.*, 1996, **2**, pp. 435–453
3 Keller, U.: 'Nonlinear optics in semiconductors', in Gaimore, E., and Kost, A. (Eds.): (Academic Press, Inc., Boston, 1999) vol. 59, Chap. 4, p. 211
4 Hönniger, C., Paschotta, R., Morier-Genoud, F., Moser, M., and Keller, U.: 'Q-switching stability limits of continuous-wave passive mode locking', *J. Opt. Soc. Am. B, Opt. Phys.*, 1999, **16**, pp. 46–56
5 Fluck, R., Zhang, G., Keller, U., Weingarten, K.J., and Moser, M.: 'Diode-pumped passively mode-locked 1.3-μm Nd:YVO_4 and Nd:YLF lasers by use of semiconductor saturable absorbers', *Opt. Lett.*, 1996, **21**, pp. 1378–1380
6 Ptak, A.J., Kurtz, S., Johnston, S.W., Friedman, D.J., Geisz, J.F., Olson, J.M., McMahon, W.E., Kibbler, A.E., Kramer, C., Young, M., Wei, S.H., Zhang, S.B., Janotti, A., Carrier, P., Crandall, R.S., Keyes, B.M., Dippo, P., Norman, A.G., Metzger, W.K., Ahrenkiel, R.K., Reedy, R.C., Gedvilas, L., To, B., Weber, M.H., and Lynn, K.G.: 'Defects in GaInNAs: what we've learned so far'. Proc. NCPV and Solar Program Review Meeting 2003, 2003, NREL/CD-520-33586, pp. 202–205
7 Kondow, M., Uomi, K., Niwa, A., Kitatani, T., Watahiki, S., and Yazawa, Y.: 'GaInNAs: a novel material for long-wavelength-range laser diodes with excellent high-temperature perfirmance', *Jpn. J. Appl. Phys.*, 1996, **35**, pp. 1273–1275
8 Riechert, H., Ramakrishnan, A., and Steinle, G.: 'Development of InGaAsN-based 1.3-μm VCSELs', *Semicond. Sci. Technol.*, 2002, **17**, pp. 892–897
9 Kondow, M., and Kitatani, T.: 'Molecular beam epitaxy of GaNAs and GaInNAs', *Semicond. Sci. Technol.*, 2002, **17**, pp. 746–754
10 Sun, H.D., Valentine, G.J., Macaluso, R., Calvez, S., Burns, D., Dawson, M.D., Jouhti, T., and Pessa, M.: 'Low-loss 1.3-μm GaInNAs saturable Bragg reflector for high-power picosecond neodymium lasers', *Opt. Lett.*, 2002, **27**, pp. 2124–2126
11 Paschotta, R., and Keller, U.: 'Passive mode locking with slow saturable absorbers', *Appl. Phys. B, Lasers Opt.*, 2001, **73**, pp. 653–662